Probabilistic tsunami inundation assessment for the maximum possible earthquake magnitude: A case study of the Sagami Trough megathrust earthquake in Japan

Y. Fukutani[(1)]

[(1)] *Associate Professor, Kanto Gakuin University, fukutani@kanto-gakuin.ac.jp*

Abstract

In Japan, the government has assumed the occurrence of the maximum possible future earthquake magnitudes along the major oceanic trenches around the country to create tsunami hazard maps to be used in evacuation planning for local residents living in coastal areas. There are various uncertainties associated with the assumption of tsunamis caused by the maximum possible earthquake magnitudes, but these uncertainties are not taken into account, and generally, only one inundation area is shown on the tsunami hazard map, which does not help local residents properly understand these uncertainties. The purpose of this study is to conduct a probabilistic tsunami inundation assessment for the maximum possible earthquake magnitude in the Sagami Trough megathrust earthquake in Japan, show the uncertainties of the assumed tsunami by performing a numerical simulation of tsunami inundation considering various uncertainties and reduce the computational costs using the mode decomposition method. First, we developed 9 cases of fault parameters of the Sagami Trough megathrust earthquake (Mw 8.7) considering these uncertainties, where the reference Mw was changed to ±0.1 and the reference fault depths were changed to -1 km and +2 km. Then, we evaluated the tsunami inundation areas and depths for all 9 cases using a nonlinear longwave equation. Next, we applied singular value decomposition to the inundation depth data and evaluated the spatial inundation modes. We can obtain a large number of possible inundation areas and probability density distributions of tsunami inundation depths in each mesh by combining these inundation modes. Finally, we obtained tsunami inundation hazard curves, which show the relationship between the tsunami inundation depth and the probability of exceedance within the next 30 years following 2021 by applying the Brownian Passage Time (BPT) distribution as the occurrence probability of the Sagami Trough earthquake and performing a time-dependent Monte Carlo simulation for 100,000 years using the probability density function of tsunami inundation depths. The proposed method can be used to evaluate the tsunami inundation area considering the uncertainty of the largest earthquake with a relatively low computational cost and could be an effective method to evaluate the uncertainty of tsunami hazard maps and the probability density function of tsunami inundation depths at each point.

Keywords: probabilistic tsunami hazard assessment; tsunami hazard map; mode decomposition method

1. Introduction

In Japan, the government has assumed the occurrence of the maximum possible future earthquake magnitude along the major oceanic trenches surrounding the country based on the results of seismic observation studies to create tsunami hazard maps to be used in evacuation planning for local residents living in coastal areas. There are various uncertainties associated with the assumption of a tsunami caused by the maximum possible earthquake magnitude, but in general, these uncertainties are not taken into account, and only one inundation area is shown on tsunami hazard maps. Based on the idea that such uncertainty should also be clearly indicated on tsunami hazard maps, the Ministry of Land, Infrastructure, Transport and Tourism (MLIT) stated that it is important to set a buffer zone outside the tsunami inundation area to be cautious by considering the actual situation of the area and taking into account the uncertainty of the hazard assessment [1]. The buffer zone is defined as the area that is not inundated according to the inundation prediction calculation but is likely to be inundated considering the uncertainty of the hazard assessment and is an important concept in designating evacuation areas. Fig. 1 shows a conceptual diagram of a buffer zone. An inundation zone is assumed in the coastal area, and a buffer zone is designated outside of the assumed inundation zone, which may be inundated given the uncertainty of the prediction. In Japan, the assumed inundation zones due to megathrust earthquakes are announced by prefectural governments, and then local governments designate tsunami hazard maps and buffer zones considering the local conditions.

However, there is no specific method for local governments to evaluate the uncertainty of hazard assessments and designate buffer zones. Some local governments have already designated buffer zones, but they have done so without clear criteria or precedents. Many other local governments have not prepared hazard maps that take into account uncertainties, including buffer zones. The 2011 Tohoku tsunami inundated areas that were far beyond the previously assumed tsunami inundation zone, which again demonstrated the uncertainty involved in hazard assessment. Therefore, it is desirable to develop a specific method for setting buffer zones as a means to clearly indicate the uncertainty of prediction on hazard maps.

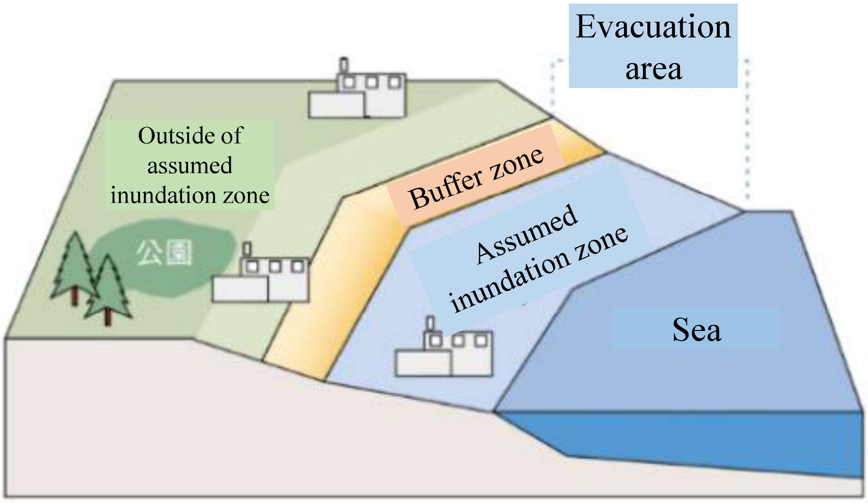

Fig. 1 – Buffer zone in a tsunami hazard map [1]

In the assessment of earthquake-induced tsunami hazards, there are many uncertainties associated with tsunami generation, propagation and run-up processes. For example, the location and shape of the seismogenic fault, the starting point of fault rupture, the rise time in the tsunami generation process, the method used to calculate the initial water level, the governing equation of the tsunami, the tide level setting, the seafloor topography in the region of tsunami propagation, the terrestrial topography, the distribution of man-made structures (e.g., buildings and seawalls) and the roughness in the tsunami run-up process all affect the final tsunami hazard assessment on land; the impact factors include the inundation depth and inundation area. In addition, the fault parameters, including the location, width, length, slip, depth, rake, strike, and dip of the fault, all of which determine the location and shape of the seismogenic fault, vary both temporally and spatially, and these variations affect the results of tsunami hazard assessments. The probabilistic tsunami hazard assessment (PTHA) method is used to evaluate such uncertainties in tsunami hazard assessments, and a variety of PTHA approaches have been proposed since the turn of the millennium (e.g., [1, 2, 3, 4, 5, 6]). In most of the previous studies, a large number of assumed earthquake faults have been generated, nonlinear longwave equations have been solved, and tsunami wave heights and inundation depths have been evaluated to obtain the hazard curves or frequency distributions of tsunami wave height or inundation depth at a certain point. However, solving such a large number of nonlinear equations imposes an enormous computational load and is not practical. In addition, once the various conditions of the simulation, such as the land and coastal topography and embankment conditions, change, it is necessary to re-evaluate, which again requires a significant computational load and is not a practical means. [5] and [7] proposed a calculation method of probabilistic tsunami inundation depth estimation with relatively low computational costs for European coastal areas using Green's function method. However, an efficient and physically valid method to evaluate the uncertainty of tsunami inundation depth is still under research.

Based on this background, the purpose of this study is to conduct probabilistic tsunami inundation assessments for the maximum possible earthquake magnitude in the Sagami Trough and to show the uncertainties of the assumed tsunami by performing numerical simulations of tsunami inundation considering various uncertainties and reducing the computational cost by using the mode decomposition method.

2. Methodology

2.1 Tsunami numerical simulation

Given the fault parameters of an earthquake that serves as the tsunami source, we evaluate the amount of crustal movement using Okada's equation [8]. Then, we obtain the initial water level of the tsunami by taking the crustal movement as the change in sea level and conduct a tsunami numerical simulation by using the following nonlinear longwave equations (continuity equation and equations of motion, Eqs. (1), (2) and (3)) [9, 10]:

$$\frac{\partial \eta}{\partial t}+\frac{\partial M}{\partial x}+\frac{\partial N}{\partial y}=0 \tag{1}$$

$$\frac{\partial M}{\partial t}+\frac{\partial}{\partial x}\left(\frac{M^2}{D}\right)+\frac{\partial}{\partial y}\left(\frac{MN}{D}\right)+gD\frac{\partial \eta}{\partial x}+\frac{gn^2 M}{D^{7/3}}\sqrt{M^2+N^2}=0 \tag{2}$$

$$\frac{\partial N}{\partial t}+\frac{\partial}{\partial x}\left(\frac{MN}{D}\right)+\frac{\partial}{\partial y}\left(\frac{N^2}{D}\right)+gD\frac{\partial \eta}{\partial y}+\frac{gn^2 N}{D^{7/3}}\sqrt{M^2+N^2}=0 \tag{3}$$

where η denotes the water level, D denotes the total water level, g denotes the acceleration due to gravity, n denotes the Manning coefficient, and M and N denote the fluxes in the x and y directions, respectively. The governing equations were discretized via the staggered leapfrog scheme.

2.2 Proper orthogonal decomposition and Surrogate model

First, the inundation depth matrix at each mesh point i calculated by the nonlinear longwave equations (Eqs. (1), (2) and (3)) is defined as $\boldsymbol{x}=(x_1,\dots,x_i)^T$. The following inundation data matrix $\boldsymbol{X}$ is generated with the number of analysis cases j considering the uncertainty of the seismogenic fault and the inundation depth value for each analysis case j as $\boldsymbol{x}_j$:

$$\boldsymbol{X}=(\boldsymbol{x}_1,\dots,\boldsymbol{x}_j)=\begin{pmatrix} x_{11} & \cdots & x_{1j} \\ \cdots & \cdots & \cdots \\ x_{i1} & \cdots & x_{ij} \end{pmatrix} \tag{4}$$

where $\boldsymbol{X}$ is an $i\times j$ matrix and is often a nonsquare matrix. We apply singular value decomposition (SVD) to this data matrix $\boldsymbol{X}$:

$$\boldsymbol{X}=\boldsymbol{U\Sigma V^T}=\begin{pmatrix} | & \cdots & | \\ \boldsymbol{u}_1 & \cdots & \boldsymbol{u}_j \\ | & \cdots & | \end{pmatrix}\begin{pmatrix} \lambda_1 & \cdots & 0 \\ \vdots & \ddots & \vdots \\ 0 & \cdots & \lambda_j \end{pmatrix}\begin{pmatrix} — & \boldsymbol{v}_1 & — \\ \vdots & \vdots & \vdots \\ — & \boldsymbol{v}_j & — \end{pmatrix}^T \tag{5}$$

where $\boldsymbol{U}$ is an $i \times j$ orthonormal matrix containing the left-singular vectors $\boldsymbol{u}_j$, $\boldsymbol{\Sigma}$ is an $j \times j$ pseudodiagonal and semipositive definite matrix with diagonal entries containing the singular values $\boldsymbol{\lambda}_j$, and $\boldsymbol{V}$ is an $j \times j$ orthonormal matrix containing the right-singular vectors $\boldsymbol{v}_j$. In relation to the covariance matrix of $\boldsymbol{X}$, the information about the spatial correlation between the meshes is aggregated into a left-singular vector $\boldsymbol{U}$ and a singular value $\boldsymbol{\Sigma}$. The left-singular vectors $\boldsymbol{u}_j$ refer to the eigenmodes j of the tsunami inundation depth distributions. From Eq. (5), the column vector $\boldsymbol{x}_j$ of inundation depths for a case j can be transformed as follows:

$$\boldsymbol{x}_j = \sum_{k=1}^{N} \boldsymbol{u}_k (\lambda_k v_{kj}^T) = \sum_{k=1}^{N} (\lambda_k v_{jk}) \boldsymbol{u}_k = \sum_{k=1}^{N} (\alpha_{jk}) \boldsymbol{u}_k \tag{6}$$

where N is the number of all modes and α_{jk} is expressed as the coefficient of the jth case for mode k multiplied by the singular value and the right-singular vector. Eq. (6) demonstrates that the column vector $\boldsymbol{x}_j$ of the inundation depth can be represented as a linear sum of each mode value. Considering the influence of each mode represented by the singular value λ, we can generate a surrogate model with reduced dimensionality by removing only the low-impact modes. The coefficient α_{jk} estimates its distribution by a Bayesian estimation technique using a Gaussian process.

A Gaussian process is a collection of random variables, any Gaussian process finite number of which has a joint Gaussian distribution [11]. First, we generate a random Gaussian vector with the zero mean and the covariance function as follows:

$$f(\boldsymbol{x}) \sim \mathcal{N}(0, k(\boldsymbol{x}, \boldsymbol{x}_*)) \tag{7}$$

We take the mean function to be zero due to a lack of prior knowledge. The covariance function $k(\boldsymbol{x}, \boldsymbol{x}_*)$, also known as the kernel function, has been proposed in many different ways depending on its application, but in this study, we utilize the commonly used Gaussian kernel. Let $f(\boldsymbol{x}) = \boldsymbol{f}$ be a function of α_{jk} corresponding to each mode obtained from SVD as the training points $\boldsymbol{x} = (x_1, \dots, x_j)$ for case j of the tsunami inundation analysis, and let $f(\boldsymbol{x}_*) = \boldsymbol{f}_*$ be the prediction function of α_{jk} for any number of n_* test points where $\boldsymbol{X}_* = (x_1^*, \dots, x_n^*)$. Then, these simultaneous distributions are calculated as follows:

$$\begin{bmatrix} \boldsymbol{f} \\ \boldsymbol{f}_* \end{bmatrix} \sim \mathcal{N}\left(0, \begin{bmatrix} K(\boldsymbol{x}, \boldsymbol{x}) & K(\boldsymbol{x}, \boldsymbol{x}_*) \\ K(\boldsymbol{x}_*, \boldsymbol{x}) & K(\boldsymbol{x}_*, \boldsymbol{x}_*) \end{bmatrix}\right) \tag{8}$$

where $K(\boldsymbol{x}, \boldsymbol{x})$ is a matrix with m and n components of the Gaussian kernel $k(x_m, x_n)$. It should be noted that we perform regression analysis by using a noise-free Gaussian process so that the estimates pass through the value of α_{jk} obtained by SVD at the data point during the tsunami inundation analysis. Using Bayesian theory, the conditional distribution $\boldsymbol{f}_*|\boldsymbol{f}$ (i.e., the posterior distribution) that follows the prediction $\boldsymbol{f}_*$ given the training function $\boldsymbol{f}$ (i.e., the prior distribution) is:

$$\boldsymbol{f}_*|\boldsymbol{f} \sim \mathcal{N}(\boldsymbol{m}_*, \boldsymbol{V}_*) \tag{9}$$

$$\boldsymbol{m}_* = K(\boldsymbol{x}, \boldsymbol{x}_*)^T K(\boldsymbol{x}, \boldsymbol{x})^{-1} \boldsymbol{f} \tag{10}$$

$$\boldsymbol{V}_* = K(\boldsymbol{x}_*, \boldsymbol{x}_*) - K(\boldsymbol{x}, \boldsymbol{x}_*)^T K(\boldsymbol{x}, \boldsymbol{x})^{-1} K(\boldsymbol{x}, \boldsymbol{x}_*) \tag{11}$$

where $\boldsymbol{m}_*$ is the expected value and $\boldsymbol{V}_*$ is the covariance function of the posterior distribution. We can generate the distribution values $\boldsymbol{f}_*$ from the joint posterior distribution by evaluating the mean and covariance functions from Eqs. (9), (10) and (11) and generate the samples accordingly.

2.3 Time-dependent occurrence probability model

To evaluate the tsunami hazard curves and probabilistic tsunami inundation depth distributions due to earthquake-induced tsunamis in a given area, it is necessary to consider the probability of each target earthquake. As explained in the Introduction, several methods have been proposed to evaluate the earthquake occurrence probability. The Sagami Trough earthquake, the target of this study, is a repeated historical event, and its interval of occurrence has been specified [12]. Therefore, we use the following time-dependent model, referred to as the BPT distribution:

$$P(t) = \sqrt{\frac{\mu}{2\pi\alpha^2 t^3}} \exp\left(-\frac{(t-\mu)^2}{2\mu\alpha^2 t}\right) \tag{12}$$

where t is the elapsed time since the last earthquake, μ and α are the first- and second-order parameters of the distribution, respectively, and μ is defined as the mean interval between active years for the earthquake. By conducting time-dependent Monte Carlo simulations using the occurrence probability model of the target earthquake represented by Eq. (12), we can conduct a PTHA in the target region for the next ΔT years.

3. Application to the Sagami Trough megathrust earthquake

The theoretical framework outlined in Chapter 2 is applied to the Sagami Trough earthquake, which is assumed to occur in the vicinity of major metropolitan areas in Japan.

3.1 Tsunami numerical simulation

In this study, we consider the uncertainties in earthquake Mw and fault depth. Fig. 2 shows the slip distribution of the generated Sagami Trough megathrust earthquake. This was generated based on the fault parameters of the Sagami Trough megathrust earthquake (western model) (Mw 8.7) published by the Cabinet Office in 2012. Using the initial water level as an input value evaluated by using the theory of Okada [8], we performed tsunami numerical simulations via nonlinear shallow water equations and the continuity equation (Eqs. (1), (2) and (3)) with a time interval of 0.6 seconds and a grid spacing of 270 m - 90 m - 30 m - 10 m. We performed tsunami numerical simulations for the first 3 hours after the earthquake so that the maximum tsunami inundation depth could be properly evaluated while considering the effects of tsunami reflection and amplification. We used the topographic and roughness data published by the Cabinet Office [13] in our numerical simulations and did not consider terrestrial structures.

Fig. 3 shows the distributions of the maximum tsunami inundation depths for the target area simulated for 9 seismogenic faults with three Mw values and three fault depths. Changes in Mw were achieved by adjusting the amount of slip. Fig. 4 shows the tsunami hazard map published by the city of Zushi. The simulation results of Fig. 3(e), which is the control case without considering the uncertainty of Mw and fault depth, and the tsunami hazard map in Fig. 4 shows almost the same inundation area, indicating that the tsunami numerical calculation is properly performed.

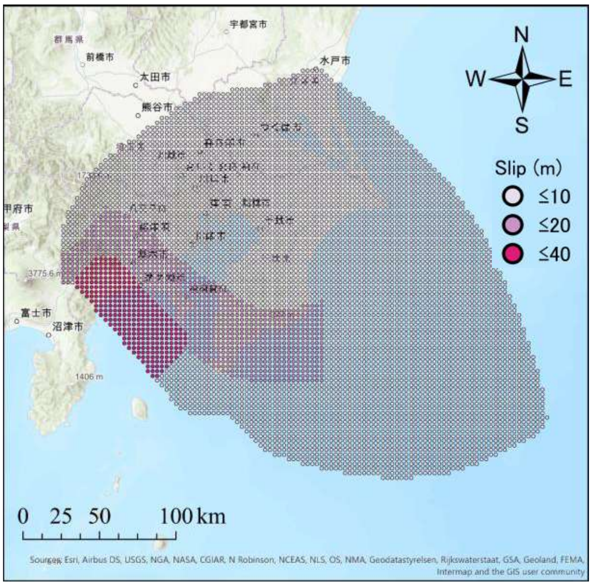

Fig. 2 – Sagami trough megathrust earthquake

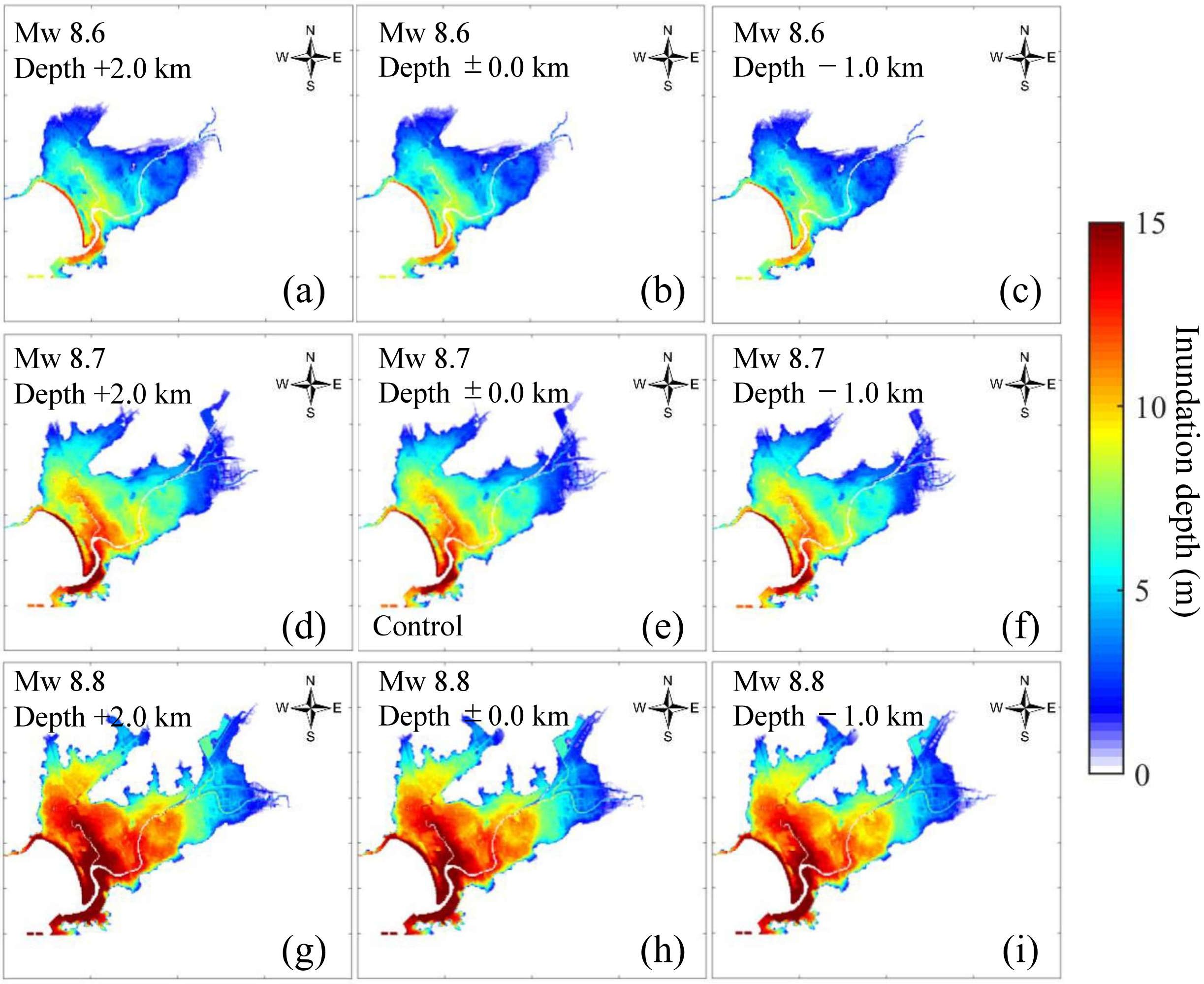

Fig. 3 – Tsunami inundation results for Zushi city, Japan

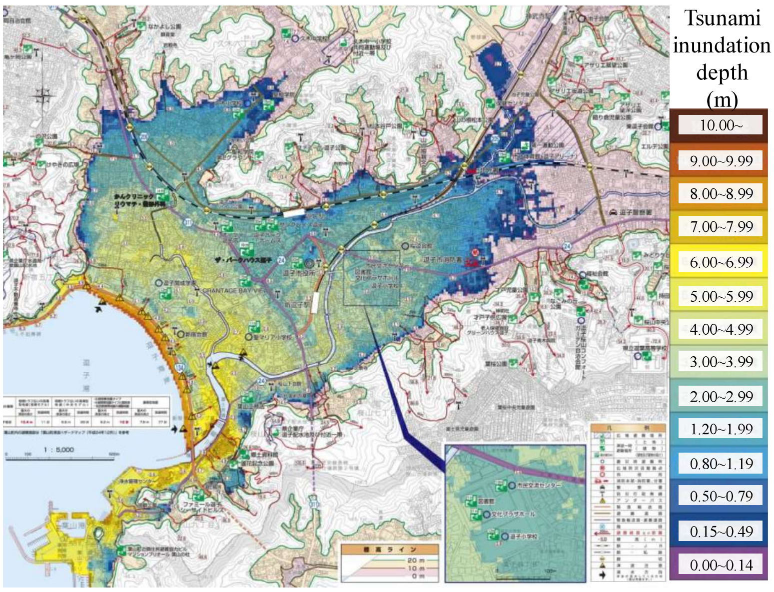

Fig. 4 – Tsunami hazard map for Zushi city, Japan

3.2 Mode decomposition and Surrogate model

We generated data matrix $\boldsymbol{X}$ for the 9 tsunami inundation depth distributions and decomposed the matrix into singular vectors. Fig. 5 shows the spatial distribution of column vectors $\boldsymbol{u}_j$ (j = 1, …, 9) comprising the left-singular vector. These column vectors are called modes, and we can identify 9 mode distributions corresponding to various tsunami inundation depths. Positive values in the figure are shown in red, while negative values are shown in blue (representing a positive correlation of the inundation depth between meshes of the same sign and a negative correlation of the inundation depth between meshes of different signs).

Fig. 6 shows the contribution rate c_j calculated in Eq. (13), where n is the number of analysis cases; thus, n = 9. We found that approximately 82.7% of the total can be represented by the first mode, 97.8% by the first through third modes, 99.0% by the first through fifth modes, and 99.7% by the first through seventh modes.

$$c_j = \frac{\lambda_j}{\sum_{k=1}^{n} \lambda_k} \tag{13}$$

Next, we estimated the coefficients α_{jk} using the Bayesian estimation method with the Gaussian process. Fig. 7 shows the coefficients α_{jk} corresponding to each mode estimated by Eqs. (8), (9) and (10). The red dots reflect the values of α_{jk} in each mode, and the tsunami numerical simulation results are fully reproduced, where the smooth surface estimated using Gaussian process regression passing through the red points is the posterior distribution $\boldsymbol{m}_*$.

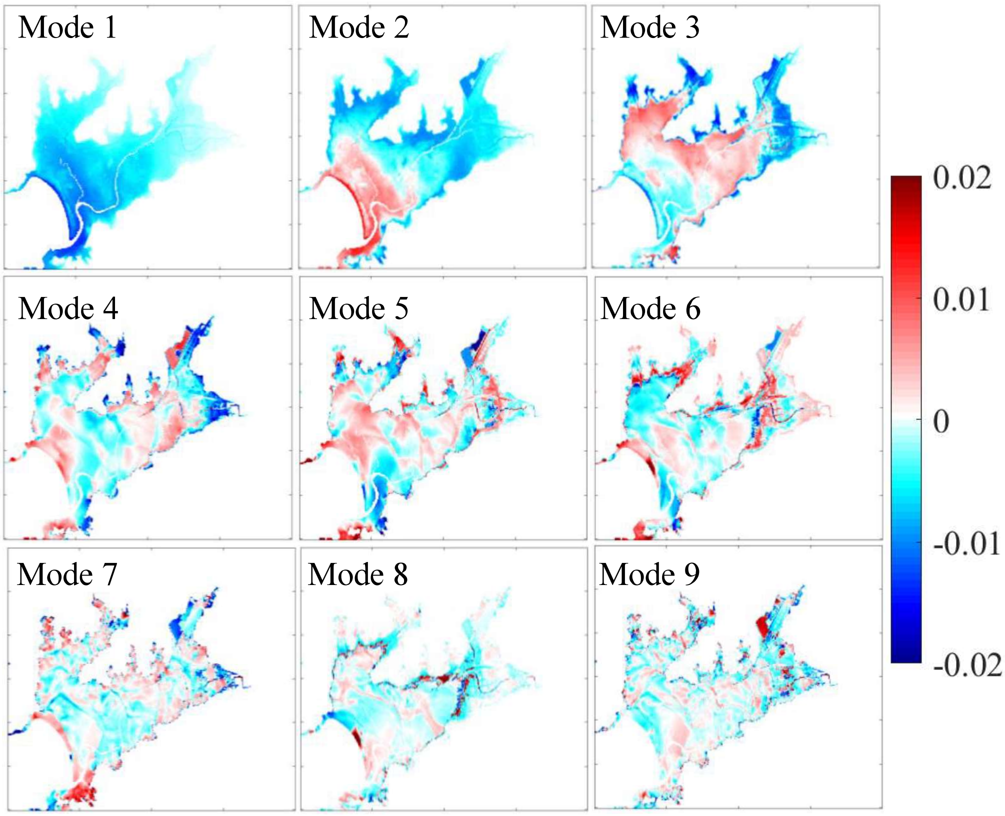

Fig. 5 – Mode decomposition results for tsunami inundation depth data

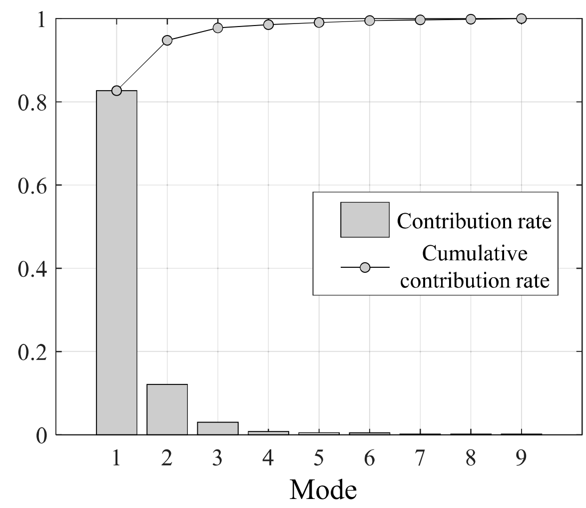

Fig. 6 – Contribution rate for each mode

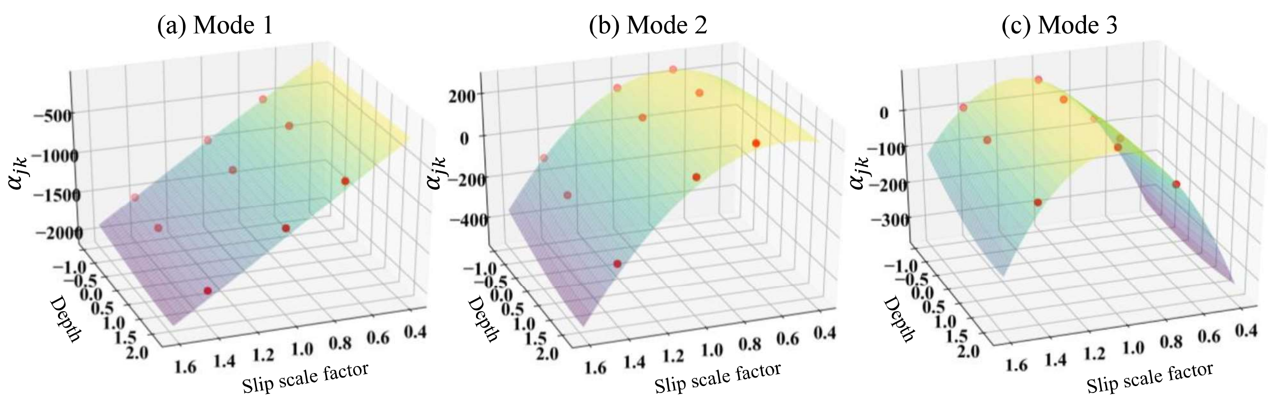

Fig. 7 – Estimates of the coefficients α_{jk} for the input parameters (slip scale factor and fault depth) using Gaussian process regression

We generated the fault depth and slip scale factor by using random numbers and took them as the input parameters. Based on the criteria of JSCE [14], which states that the slip amount of a seismogenic fault should include an error of approximately ±0.1 for Mw when considering previous earthquakes within the same area, we established a lognormal distribution with a mean of 1.0 and a log standard deviation of 0.35 so that Mw varied by ±0.1. Then, we evaluated the fault depth with a normal distribution (mean of ±0.0 km and standard deviation of 2.0 km). The standard deviation was set to 2.0 km in this study based on the report of the Earthquake Research Institute [15], which reported the depth to the upper boundary of the Philippine Sea plate. The degrees of uncertainty in these parameters should be evaluated in a variable manner depending on the recently acquired knowledge about seismogenic faults and tectonic plates.

We determined the coefficients α_{jk} using random numbers following the abovementioned probability distribution of the input parameters and randomly generated the inundation depth distribution using the surrogate model represented by Eq. (6). Fig. 8(a) shows the average inundation depth in each mesh evaluated by using 10,000 random numbers, and Fig. 8(b) shows the maximum inundation depth in each mesh sampled with 10,000 simulations. The mean values in Fig. 8(a) are similar to the inundation depth distribution for the control case in Fig. 3(e), and the maximum values in Fig. 8(b) are similar to the inundation depth distribution for the Mw 8.8 case in Fig. 7(g), (h) and (i), indicating that we were able to reproduce the spatial distribution of tsunami inundation depths produced from the numerical analysis by using the surrogate model. Fig. 8(c) shows the standard deviation of tsunami inundation depth. This allows us to understand the characteristics of the variability of the tsunami inundation depth.

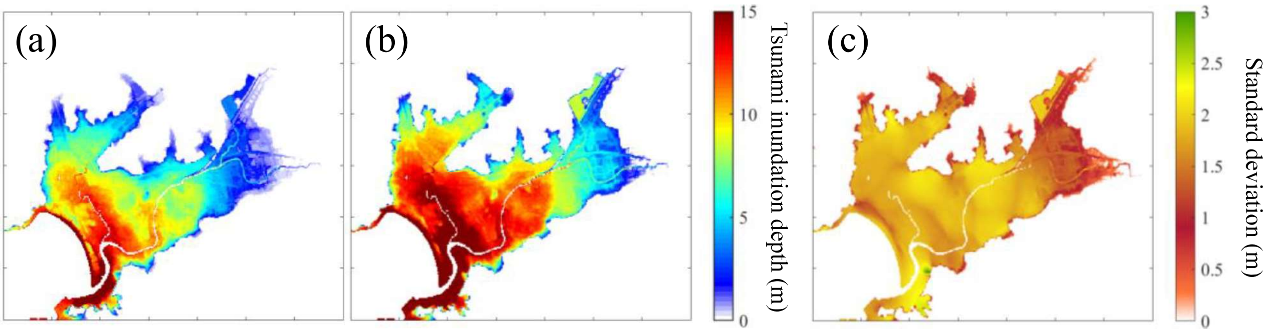

Fig. 8 – (a) Average, (b) maximum and (c) standard deviation of the tsunami inundation depth by Monte Carlo simulation results

3.3 Tsunami inundation hazard curves

Finally, we obtained tsunami inundation hazard curves (see Fig. 9), which show the relationship between the tsunami inundation depth and the probability of exceedance within the next 30 years from 2021 by applying the Brownian Passage Time (BPT) distribution as the occurrence probability of the Sagami Trough earthquake and performing a time-dependent Monte Carlo simulation for 100,000 years using the probability density function of the tsunami inundation depths.

The Earthquake Research Committee [12] assessed the probability of an M8-class earthquake in the Sagami Trough region from multiple perspectives and ultimately estimated that the average interval between earthquakes is 180 to 590 years based on topographic and geological data. They estimated the value of α in the BPT distribution to represent the variability of the earthquake interval as α = 0.24 by using the maximum likelihood method and referencing the value used in the evaluation of active faults. Fig. 9 shows the calculated tsunami hazard curves at a point in the city of Zushi for the four cases of α = 0.24, α = 0.20, μ = 180 and μ = 250. The setting of parameters α and μ has a great influence on the evaluation results of the hazard curve. By implementing the above procedure for each computational mesh, for example, we can evaluate the tsunami inundation area for each return period (e.g., 100 years, 1000 years), but this calculation will be performed in future studies.

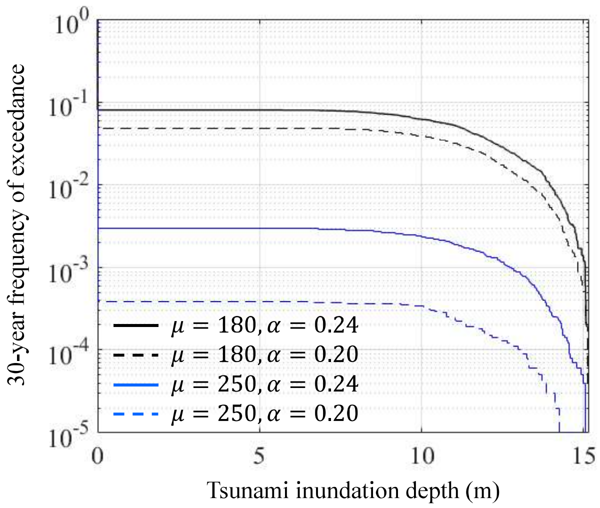

Fig. 9 – Average and maximum inundation depth of the simulation results

The probabilistic tsunami inundation assessment method using proper orthogonal decomposition is expected to be used as a buffer zone setting method for tsunami hazard maps. For example, the tsunami inundation area for each return period, such as 1,000 years or 2,500 years calculated by this method, may be designated as a buffer zone. A tsunami with a return period of 2,500 years is defined as the maximum considered tsunami (MCT) in the ASCE. Another possibility is to adopt the maximum inundation area evaluated by the Monte Carlo simulation (Fig. 8(b)).

4. Conclusion

We proposed a probabilistic tsunami inundation assessment method using proper orthogonal decomposition as a method to determine the buffer zone for tsunami hazard maps to be set up by local governments in Japan. The current tsunami hazard maps are prepared for the largest class of earthquakes, and this method can be effective when considering the uncertainty of tsunami hazards from the largest class of earthquakes. By applying this method to various earthquakes, a complete probabilistic tsunami inundation assessment can be carried out. According to the results of the questionnaire survey to the local governments, setting buffer zones for tsunami hazard maps is not a simple matter because it cannot be done by only considering the uncertainty of the hazard but also needs to be done after careful consideration that reflects the intentions of the residents living in the area. However, a reliable assessment will be possible if the method in this study is first used to examine the uncertainty of the hazard, followed by discussions among local governments, local residents, and experts based on the results of the study, and finally the designation of buffer zones.

5. Acknowledgments

We thank the anonymous reviewers who provided us with valuable comments and helped improve the manuscript. This research was partially supported by JSPS KAKENHI Grant Number JP19K15266 and funding from the Nuclear Safety Research Institute, Chubu Electric Power Co., Inc.

6. References

[1] Ministry of Land, Infrastructure, Transport and Tourism (2004): Outline of the Tsunami and Storm Surge Hazard Map Manual (in Japanese). http://www.mlit.go.jp/common/000054428.pdf.

[2] Geist E (2002): Complex earthquake rupture and local tsunami. *Journal of Geophysical Research*, **107**, ESE2-1-ESE2-15. https://doi.org/10.1029/2000JB000139.

[3] Geist E, Parsons T (2006): Probabilistic analysis of Tsunami Hazards. *Natural Hazards*, **37**, 277-314. https://doi.org/10.1007/s11069-005-4646-z.

[4] Gonz´alez FI, Geist EL, Jaffe B, Kânoğlu U, Mofjeld H, Synolakis CE, Titov VV, Arcas D, Bellomo D, Carlton D, Horning T, Johnson J, Newman J, Parsons T, Peters R, Peterson C, Priest G, Venturato A, Weber J, Wong F, Yalcine A (2009): Probabilistic tsunami hazard assessment at Seaside, Oregon, for near- and far-field seismic sources. *Journal of Geophysical Research*, **114**, C11023. https://doi.org/10.1029/2008JC005132.

[5] Grezio A, Babeyko A, Baptista MA, Behrens J, Costa A, Davies G, et al (2017): Probabilistic tsunami hazard analysis: Multiple sources and global applications. *Reviews of Geophysics*, **55** (4), 1158-1198. https://doi.org/10.1002/2017RG000579.

[6] Mori N, Goda K, Cox D (2018): Recent process in probabilistic tsunami hazard analysis (PTHA) for mega thrust subduction earthquakes. In V. Santiago-Fandiño, Sato S, Maki N, Iuchi K (Eds.), The 2011 Japan earthquake and tsunami: Reconstruction and restoration: Insights and assessment after 5 years (pp. 469-485). Cham, Switzerland: Springer International Publishing.

[7] Glimsdal S, Løvholt F, Harbitz C, Romano F, Lorito S, Orefice S, et al (2019): A new approximate method for quantifying tsunami maximum inundation height probability. *Pure and Applied Geophysics*, **176**, 3227-3246. https://doi.org/10.1007/s00024-019-02091-w.

[8] Okada Y (1985): Surface deformation due to shear and tensile faults in a half-space. *Bulletin of the Seismological Society of America*, **75** (4), 1135-1154.

[9] Goto C, Ogawa Y (1982): Tsunami numerical simulation with Leap-frog scheme. Sendai, Japan: Tohoku University.

[10] UNESCO, IUGG/IOC Time Project (1997): Numerical method of tsunami simulation with the leap-flog scheme. IOC Manuals and Guides No. 35. Paris, France: UNESCO.

[11] Rasmussen CE, Williams CKI (2006): Gaussian processes for machine learning. Cambridge, MA: MIT Press.

[12] Earthquake Research Committee (2014): Long-term evaluation of seismicity along Sagami Trough (2nd version) (in Japanese), *Headquarters for Earthquake Research Promotion*, p. 81. Retrieved from https://www.jishin.go.jp/main/chousa/14apr_sagami/.

[13] Cabinet Office (2013): The committee of the model for Tokyo Metropolitan Earthquake (in Japanese). Retrieved from http://www.bousai.go.jp/kaigirep/chuobou/senmon/shutochokkajishinmodel/.

[14] Japan Society of Civil Engineers (2016): The method of tsunami risk assessment for nuclear power plants (in Japanese). Retrieved from https://committees.jsce.or.jp/ceofnp/node/84.

[15] Earthquake Research Institute, University of Tokyo, National Research Institute for Earth Science and Disaster Resilience, Disaster Prevention Research Institute, Kyoto University (2012): Special project for mitigation of Metropolitan Earthquakes (in Japanese). Retrieved from http://www.eri.u-tokyo.ac.jp/shuto/report/soukatsu/0120327.pdf.

